Heterodinuclear Ln–Na Complexes with an Asymmetric Macrocyclic Compartmental Schiff Base

Mauro Botta,*[a] Umberto Casellato,[b] Cristina Scalco,[b] Sergio Tamburini,*[b] Patrizia Tomasin,[b] Pietro A. Vigato,[b] Silvio Aime,[c] and Alessandro Barge[c]

Abstract: Heterodinuclear lanthanide(III)–sodium(I) complexes [LnNa(L)-$(Cl)_2(CH_3OH)$] (Ln = La–Nd, Sm–Lu), where H_2L is a [1+1] asymmetric compartmental macrocyclic ligand containing a N_3O_2 Schiff base and a O_3O_2 crown-ether-like coordination site, have been prepared and characterized by IR, ^1H, ^{13}C, and ^{23}Na NMR spectroscopy, mass spectrometry, and electron microscopy. In the solid state, the lanthanide(III) ions coordinate the Schiff-base N_3O_2 site, and the sodium ion occupies the O_3O_2 crownlike cavity, as shown by the X-ray crystal structures of the Nd, Eu, Gd, and Yb derivatives. In these complexes, the lanthanide(III) ion is coordinated by two chlorine atoms in the *trans* position and by three nitrogen and two negatively charged phenol oxygen atoms of the Schiff base, and the ion is heptacoordinated with a pentagonal bipyramidal geometry. The sodium ion is coordinated by three etheric oxygen atoms and the two phenolic oxygens that act as a bridge. A methanol molecule is also coordinated in the apical position of the resulting pentagonal pyramidal polyhedron. A detailed ^1H and ^{13}C NMR study was carried out in CD_3OD for both diamagnetic and paramagnetic heterodinuclear complexes [LnNa(L)$(Cl)_2(CH_3OH)$]. The complexes are also isostructural in solution, and their structures parallel those found in the solid state. Moreover, some significative distances determined in the solid state and in solution are comparable. Finally, the potential use of these complexes as molecular probes for the selective recognition of specific metal ions has been tested. In particular, their ability to act as shift reagents and the selectivity of the O_3O_2 site towards Li^+, Ca^{2+}, and K^+ were investigated by ^{23}Na NMR spectroscopy.

Keywords: lanthanides · macrocyclic ligands · Schiff bases · shift reagents · sodium

Introduction

In the last two decades, considerable efforts have been made to design and synthesize compartmental macrocyclic systems, owing to their well-known ability to secure, in close proximity, two metal ions in well-defined structural environments.[1–4] The compartmental macrocyclic complexes may provide unique routes to highly selective molecular recognition processes as well as to a number of peculiar physico-chemical properties.[5–7] In the early studies, [2+2] symmetric tetraimine cyclic Schiff bases, prepared by one-step condensation of 2,6-diformyl-4-substituted derivatives with appropriate diamines in the presence of suitable metal ions as templating agents, were used. These symmetric Robson-type macrocycles, owing to the identity of the two adjacent chambers, form almost exclusively homodinuclear complexes.[8–12] Heterodinuclear complexation is also possible under particularly favorable experimental conditions, which allow the formation of a well-defined mononuclear complex to be used as a ligand for further heterocomplexation.[13–15] However, this synthetic strategy can give rise to a number of scrambling reactions, with the formation of a mixture of positional isomers, of homodinuclear complexes, and so on.

More recently, in order to overcome these problems, asymmetric compartmental ligands have been designed, and their coordination ability towards different metal ions has been extensively investigated. A marked difference in the set

---

[a] Prof. M. Botta
Dipartimento di Scienze e Tecnologie Avanzate
Università del Piemonte Orientale "Amedeo Avogadro"
Corso Borsalino 54, 15100 Alessandria (Italy)
Fax: (+390) 11-6707855
E-mail: mauro.botta@unito.it

[b] Dr. S. Tamburini, Dr. U. Casellato, Dr. C. Scalco, Dr. P. Tomasin, Dr. P. A. Vigato
Istituto di Chimica Inorganica e delle Superfici
C.N.R., Padova (Italy)
Fax: (+390) 49/8702911
E-mail: tamburini@icis.cnr.it

[c] Prof. S. Aime, Dr. A. Barge
Dipartimento di Chimica I.F.M., Università di Torino
Via P. Giuria 7, 10125 Torino (Italy)

Supporting information for this article is available on the WWW under http://www.chemeurj.org/ or from the author. Listing of chemical shifts (δ/ppm; 90 MHz), paramagnetic contribution to the longitudinal relaxation rates (R_{1p} s^{-1}) at 90, 270, and 400 MHz, and calculated Yb–H distance values for the ^1H NMR spectrum of $[YbNa(L)]^{2+}$ in CD_3OD at 303 K (Table S1) are given.

of donor atoms of the two adjacent chambers favors the formation of heterodinuclear complexes rather than homodinuclear ones, and thus this limits considerably the possibility of positional heterodinuclear isomers.[2, 16] It is expected that the resulting heterodinuclear metal-ion association can yield significative mutual interactions, which may be exploited for applications in different areas of chemical research.[2, 3, 7, 17–21] Schiff bases have been extensively used in the design of coordination systems capable of securing lanthanide(III) or transition-metal ions. Moreover, crown ethers have been specially designed for Group IA and IIA metal ions. Compartmental ligands containing a Schiff base and a crown-ether moiety fused together may then provide interesting coordination possibilities. In this direction, a number of heterodinuclear complexes have been prepared and fully characterized by X-ray diffractometry.[6, 22–29] Furthermore, several molecular devices, based on such recognition capability, have been proposed.

The alkali-metal cations Na^+ and K^+ and the alkaline-earth-metal cations Mg^{2+} and Ca^{2+} are ubiquitous in living systems. The role of sodium and potassium ions stems essentially from their unequal distributions in the intra- and extracellular compartments and related transmembrane transport processes. The divalent magnesium and calcium cations possess a more marked binding ability towards macromolecules, polyelectrolytes, and biological surfaces, and thus their role is more differentiated. In the form of aqua complexes, Mg^{2+} is concentrated in the cells whereas Ca^{2+} is excluded. The distribution of alkali- and alkaline-earth-metal ions in the inner and outer cell compartments is crucial to the viability of any organism. Thus their qualitative and quantitative determination is essential, and NMR spectroscopy offers unique tools to reach this goal. The separation of the NMR signals from the two compartments is possible when their magnetic environments are made different by the presence of a paramagnetic agent, which selectively distributes in one compartment only. A successful separation of in and out signals is strongly dependent upon the interaction that the cation of interest is able to set up with the paramagnetic agent. In this context, compartmental ligands can be very useful. In fact, one may design systems containing in one chamber a suitable lanthanide(III) ion endowed with a high magnetic moment and a non-S electronic configuration, whereas the second chamber is available for coordination of an alkali- or alkaline-earth-metal ion, which is possibly involved in an exchange process with the free ions.

Using this procedure, quite interesting and powerful shift reagents have been proposed, in particular for Na^+.[20, 30] The lanthanide(III) ions offer the unique possibility of modifying progressively their physical properties (and hence their ability to act as shift reagents) while maintaining the same chemical properties. In previous investigations, it was found that the asymmetric macrocyclic ligand H_2L (Scheme 1), derived by the condensation of 3,3′-(3-oxapentane-1,5-diyldioxy)bis(2-hydroxybenzaldehyde) with 1,5-diamino-3-azamethylpentane, containing a N_3O_2 Schiff-base chamber and a O_2O_2 crown-ether-like moiety when reacted with lanthanide(III) salts, coordinates the metal ion in the crown-ether chamber rather than in the N_3O_2 Schiff base.[25, 27] X-ray diffractometric investigations of $[Ln(H_2L)(H_2O)_4](Cl)_3 \cdot nH_2O$ (Ln = Ce, Dy, $n = 1$; Ln = Lu, $n = 3$) showed that the coordination number of nine for Ln^{III} is reached by bonding five oxygen atoms from the ligand and four oxygen atoms from water molecules.[25]

It is well documented that alkali-metal ions coordinate crown ethers quite well, and in fact the same crown-ether chamber is involved in the coordination of alkali-metal ions in the case of the complexes with H_2L.[31, 32] Thus, although both ions prefer coordination at the O_2O_3 chamber, we surmise that the use of the Na^+-containing complex may force the coordination of the lanthanide(III) ion in the Schiff-base chamber. This synthetic strategy was successfully pursued, and here we report the synthesis and characterization of heterodinuclear lanthanide(III)–sodium(I) complexes with the asymmetric compartmental ligand H_2L. Furthermore, detailed NMR studies were carried out in order to assess the solution behavior of these complexes. A brief account of the Yb^{III} derivative has been recently published in a preliminary communication.[33]

Results and Discussion

Preparation and properties of the compounds: The H_2L [1+1] macrocyclic ligand and its homo- and heterodinuclear complexes have been prepared according to Scheme 1. The diformyl precursor 3,3′-(3-oxapentane-1,5-diyldioxy)bis(2-hydroxybenzaldehyde), H_2L', and its related disodium derivative Na_2L' were prepared as pale yellow solids, stable in air and soluble in organic solvents, by the reaction of the appropriate ditosylate with 2,3-dihydroxybenzaldehyde in anhydrous dimethylsulfoxide and in the presence of NaH. Pure H_2L' has been obtained by chromatography on silica gel with $CHCl_3$ as eluant. The IR spectrum of H_2L' shows a strong $\nu(C{=}O)$ at 1659–1646 cm^{-1}. The ^1H NMR ($CDCl_3$) spectrum consists of a singlet at 9.94 ppm, due to $CH{=}O$ protons, a singlet at 10.96 ppm assigned to the phenolic oxygens, multiplets at 7.15, 4.26, and 3.96 ppm associated with the aromatic and the aliphatic protons of the crown-ether chain, respectively. The IR and ^1H NMR spectra of Na_2L' parallel those of H_2L'.

The [1+1] macrocyclic ligand H_2L has been synthesized by self-condensation in methanol of H_2L' with 1,5-diamino-3-azamethylpentane (1:1 molar ratio). Alternatively, H_2L can be obtained by the same condensation reaction in the presence of $Ba(ClO_4)_2$ as a templating agent. By following this route, the yellow [1+1] macrocylic complex $[Ba(H_2L)](ClO_4)_2$ has been demetalated by guanidinium sulfate, and the resulting macrocycle H_2L extracted from water with $CHCl_3$. Finally H_2L can be conveniently prepared in high yield by the condensation of H_2L' and 1,5-diamino-3-azamethylpentane in diethyl ether by using the high-dilution technique. The latter synthetic route is the chosen method as it gives the macrocyclic ligand in high yield without the need of any further purification. H_2L is a yellow solid; its [1+1] cyclic nature was inferred by the presence of the parent peak $[M^+ - H]$ at m/z 428 in the mass spectrum and by the presence of a strong $\nu(C{=}N)$ band in the IR spectrum at 1634 cm^{-1}, whereas the bands attributable to $\nu(C{=}O)$ or $\nu(NH_2)$ completely disap-

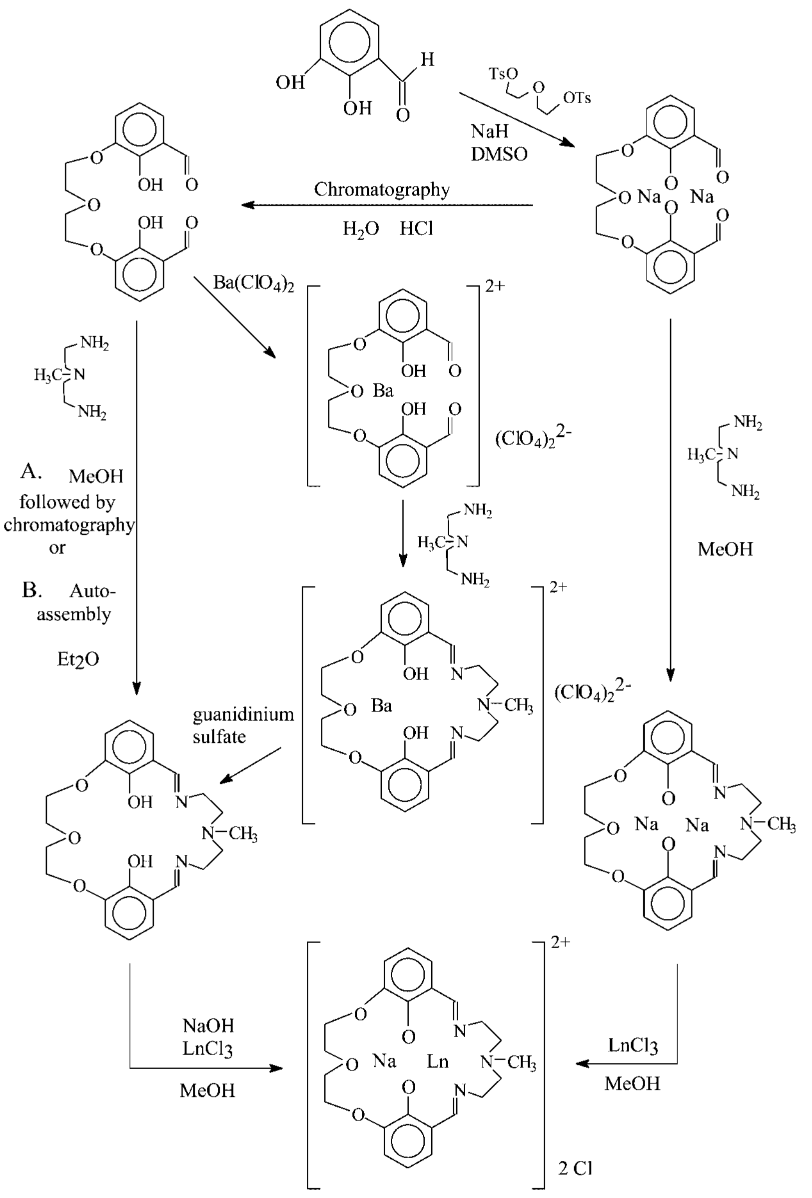

[Ln= Y, Nd, Sm, Eu, Gd, Tb, Dy, Ho, Er, Tm, Yb, Lu, La, Ce]

Scheme 1. Synthesis of the ligand H_2L and the Ln^{III} complexes.

pear. Moreover the ^1H NMR spectrum in $CDCl_3$ shows a singlet at 8.19 ppm for the iminic protons, multiplets at 6.75 ppm for the aromatic protons, at 4.20 and 3.95 ppm assigned to the methylenic protons of the crown-ether chain, at 3.63 and 2.78 ppm due to methylenic protons of the iminic chain, and a singlet at 2.32 ppm for the methyl group. The ^1H NMR spectrum of Na_2L, obtained from the condensation of the acyclic derivative Na_2L' with $H_2N(CH_2)_2N(CH_3)(CH_2)_2NH_2$, shows significative differences from H_2L owing to the coordination of the Na^+ ions in the N_3O_2 and O_3O_2 coordination chambers. As mentioned above, the reaction of H_2L with $LnCl_3 \cdot nH_2O$ in alcoholic solution gives rise to the mononuclear complex $[Ln(H_2L)(H_2O)_4](Cl)_3$. The condensation of H_2L' with 1,5-diamino-3-azamethylpentane, in the presence of $LnCl_3 \cdot nH_2O$ as templating agent, forms the same mononuclear complex. In these complexes, the lanthanide(III) ion invariably self-coordinates in the O_3O_2 chamber. The mononuclear complexes $[Ln(H_2L)((H_2O)_4]Cl)_3$ have a free N_3O_2 chamber, which is potentially available for further metal-ion complexation. However, the reaction of these complexes with alkali- or alkali-earth-metal salts gives rise to heterodinuclear complexes, which are not very stable in solution. This is possibly due to an imperfect fit of the ionic radius of Na^+ in the N_3O_2 chamber; the Na^+ in fact does not enter into the N_3O_2 plane but remains above it and is hence weakly coordinated. As a consequence, the chemical shift of ^{23}Na is very small also when strong paramagnetic lanthanide(III) ions coordinate the crown-ether O_3O_2 site.

Thus we have pursued the synthesis of positional isomers, in which the O_3O_2 site is occupied by an alkali-metal ion (i.e. Na^+), and the N_3O_2 chamber is occupied by a 4f ion in order to increase the stability of these heterodinuclear complexes and to enhance the mutual metal–metal interactions. Quite simply, we thought that the occupancy of the O_3O_2 site by a Na^+ ion would force the Ln^{III} ion to fill the Schiff-base N_3O_2 site. Thus by reacting Na_2L with the appropriate lanthanide(III) trichloride in methanol and in 1:1 molar ratio, the heterodinuclear complexes $[LnNa(L)(Cl)_2(CH_3OH)]$ are obtained. Alternatively, the macrocycle H_2L can be treated with NaOH, and the subsequent addition of $LnCl_3$ yields the same heterodinuclear complexes $[LnNa(L)(Cl)_2(CH_3OH)]$. The complexes are yellow solids, stable in the solid state and in solution, which yield well-formed crystals when recrystallized from alcoholic solution. The homogeneity of the obtained crystals and the occurrence of the correct Ln/Na/Cl ratio (1:1:2) have been checked by electron microscopy and EDX (energy-dispersive X-ray) analysis. As an example, the BSE (backscattering electrons) micrography and the EDX spectrum of the complex $[DyNa(L)(Cl)_2(CH_3OH)]$ are given in Figure 1.

The IR spectra of $[LnNa(L)(Cl)_2(CH_3OH)]$ show a lower value of ν(C=N) at 1617–1632 cm^{-1} compared with that of the free ligand (1634 cm^{-1}). Noticeably, the ν(C=N) lies at 1635–1660 cm^{-1} for the mononuclear complexes $[Ln(H_2L)(H_2O)_4](Cl)_3$ in which Ln^{3+} occupies the O_3O_2 site,

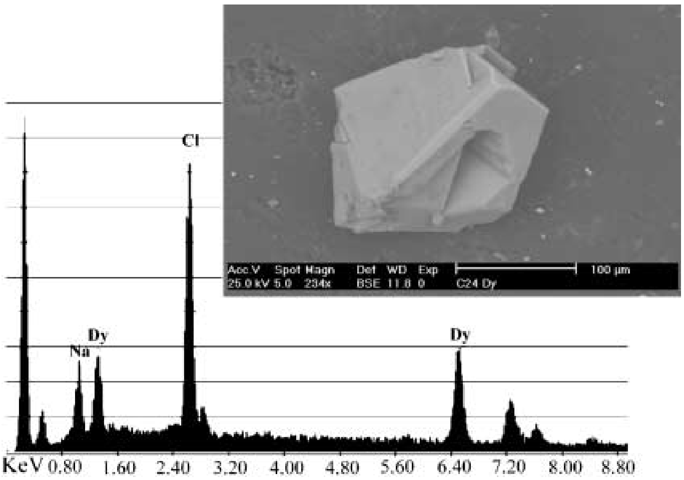

Figure 1. SEM and EDX analyses of the complex $[DyNa(L)(Cl)_2(CH_3OH)]$.

with a relevant shift ($\Delta\nu = 29 - 38\,cm^{-1}$) towards higher wavelengths compared with those for H_2L. The IR differences in the C=N stretching frequencies are clearly related to the change in the coordination mode of the lanthanide(III) ion on going from the mononuclear to the heterodinuclear complex.

X-ray structure of the heterodinuclear complexes: Crystals, grown by slow diffusion of diethyl ether into a methanolic solution of the appropriate complex, are monoclinic (space group $P2_1/n$) with four molecules in the unit cell (Table 1). The complexes $[LnNa(L)(Cl)_2(CH_3OH)]$ (Ln = Nd, Eu, Gd, Yb) are isostructural. Only the ORTEP representation of the crystal structure of the Nd complex is shown in Figure 2. The two positions of the methanol oxygen atom are indicated.

The cyclic ligand coordinates the lanthanide(III) ion in the N_3O_2 chamber and the sodium ion in the O_2O_3 one. The heptacoordination around the lanthanide(III) ion is obtained by two chloride ions, *trans* to each other, by two phenolic oxygens (also involved in the coordination of the sodium ion), and three nitrogens of the Schiff-base chamber in an equatorial plane. The resulting coordination polyhedron can be best described as a pentagonal bipyramid with the two chlorine atoms in the apical position. As for other complexes with similar cyclic ligands, the molecule adopts a butterfly shape with the two benzene rings as wings that are not symmetric in relation to the mean plane containing the five donor atoms bonded to the lanthanide ion: O1, O2, N1, N2, and N3. In fact the dihedral angle is of about 11° (mean of the four values) for the ring C1–C6 and about 32° (mean) for the ring C14–C19. The lanthanide ions are displaced from the mean basal plane: 0.099 Å for Nd, 0.072 Å for Eu, 0.070 Å for Gd, and 0.040 Å for Yb. The two apical chlorine atoms are symmetrically disposed along an axis perpendicular (176°) to the mean basal plane. Some differences in the coordination

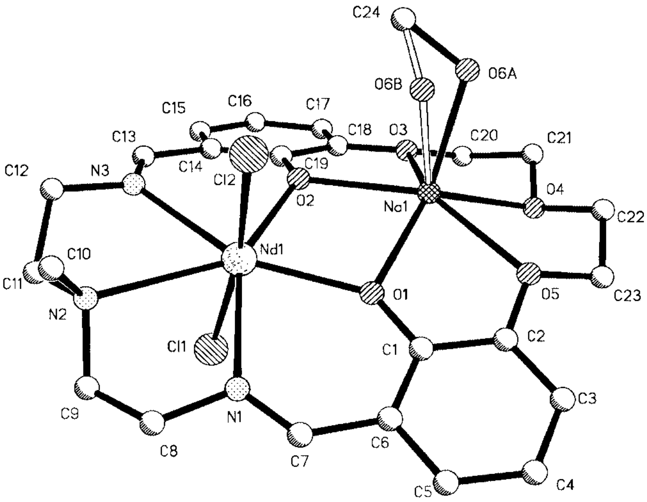

Figure 2. ORTEP diagram of $[NdNa(L)(Cl)_2(CH_3OH)]$ showing the atom-labeling scheme.

Table 1. Crystal and intensity data for Nd, Eu, Gd, and Yb complexes.

Coordinated metal	Nd	Eu	Gd	Yb
formula	$C_{24}H_{30}N_3O_6Cl_2NaNd$	$C_{24}H_{30}N_3O_6Cl_2NaEu$	$C_{24}H_{30}N_3O_6Cl_2NaGd$	$C_{24}H_{30}N_3O_6Cl_2NaYb$
unit cell	monoclinic			
space group	$P2_1/n$ (No. 14)			
a [Å]	12.567(3)	12.547(3)	12.556(4)	12.586(3)
b [Å]	13.267(4)	13.241(3)	13.236(4)	13.127(3)
c [Å]	16.769(4)	16.779(4)	16.822(5)	16.690(3)
β [°]	100.6(4)	100.4(5)	100.43(5)	101.08(3)
V [Å^3]	2757(1)	2741(1)	3315(2)	2706(1)
Z	4			
ρ [g cm^{-3}]	1.616	1.644	1.652	1.776
absorption μ [mm^{-1}] ($Mo_{K\alpha}$)	2.13	2.53	2.66	3.713
range of relat. transmission factor[a] [%]	91–100	88–100	89–100	88–100
scanned θ [°]	$6.1 \leq \theta \leq 52$	$6.1 \leq \theta \leq 60$	$6.1 \leq \theta \leq 52$	$6.2 \leq \theta \leq 60$
total/unique refl.	4050/3883	5568/5299	4426/4268	7338/7038
data observed	3849 [$F \geq 3\sigma(F)$]	5163 [$F \geq 3\sigma(F)$]	4209 [$F \geq 3\sigma(F)$]	6903 [$F \geq 3\sigma(F)$]
parameters (observ. per param.)	306 (12.5)	306 (16.9)	306 (13.7)	306 (22.5)
R_{obs}	0.038	0.035	0.054	0.041
wR (all)	0.101	0.096	0.153	0.120
highest map resid. [e Å^{-3}]	0.80	1.13	2.96	2.17
CCDC number	172974	172972	172973	172975

[a] Corrections: Lorentz polarization and absorption (empirical, ψ scan).

Table 2. Bond lengths [Å] of lanthanide- and sodium-ion coordination polyhedra.

donor atom	Ln^{III}				Na^{I}			
	Nd	Eu	Gd	Yb	Nd complex	Eu complex	Gd complex	Yb complex
Cl1	2.722(2)	2.674(1)	2.661(2)	2.583(1)				
Cl2	2.770(2)	2.729(2)	2.718(2)	2.638(1)				
O1	2.298(5)	2.266(3)	2.268(4)	2.204(3)	2.372(5)	2.362(4)	2.351(5)	2.343(4)
O2	2.319(4)	2.286(3)	2.285(4)	2.226(3)	2.339(5)	2.330(4)	2.325(5)	2.296(4)
N1	2.554(6)	2.520(4)	2.519(6)	2.459(4)				
N2	2.678(5)	2.643(4)	2.643(5)	2.593(4)				
N3	2.571(6)	2.538(4)	2.532(6)	2.470(4)				
O3					2.394(5)	2.388(4)	2.387(6)	2.370(5)
O4					2.394(5)	2.408(4)	2.423(5)	2.444(5)
O5					2.372(5)	2.355(4)	2.364(6)	2.316(4)
O6 (mean)					2.31	2.31	2.34	2.39
M···Na contact	3.552(2)	3.555(2)	3.560(3)	3.540(2)				

bonds to lanthanide ions are observed that are the direct consequence of the decrease of the ionic radius across the lanthanide series (Nd^{3+}: 0.995 Å; Eu^{3+}: 0.950 Å; Gd^{3+}: 0.938 Å; Yb^{3+}: 0.858 Å). In Table 2 we report representative bond lengths between the central metal ion and the donor atoms of the coordination sphere. A regular decrease of the bond lengths is observed: the Ln–Cl bond lengths decrease by about 0.13 Å (Nd–Cl: 2.746 Å, mean; Yb–Cl: 2.160 Å, mean), whereas for the Ln–O and Ln–N bond lengths the differences are of about 0.1 Å. On the other hand, the corresponding angles (Table 3) are not influenced by the lanthanide contraction, apart from the bridging oxygen atoms: the angle O1–Ln–O2 decreases from 80.7° for the Nd complex to 77.8° for Yb. As a direct consequence, the O1–Na–O2 angle decreases from 78.8° for the Nd complex to 73.3° for the Yb complex.

Table 3. Selected bond angles [°] of lanthanide- and sodium-ion coordination polyhedra.

	Ln^{III}			
	Nd	Eu	Gd	Yb
Cl1–M–Cl2	172.22(5)	172.30(4)	172.40(6)	172.14(4)
O1–M–O2	80.7(2)	79.7(1)	79.0(2)	77.8(1)
O1–M–N1	72.9(2)	73.7(1)	74.2(2)	74.9(1)
N2–M–N1	67.7(2)	67.7(1)	67.8(2)	67.6(1)
N2–M–N3	67.1(2)	67.7(1)	67.7(2)	67.8(1)
O2–M–N3	72.2(2)	72.1(1)	72.2(2)	73.1(1)
O1–Na–O2	78.8(2)	76.9(1)	76.6(2)	73.7(1)
O2–Na–O3	67.3(2)	67.9(1)	68.2(2)	68.7(1)
O3–Na–O4	67.4(2)	67.1(1)	66.7(2)	65.7(2)
O4–Na–O5	67.5(2)	67.4(1)	67.2(2)	67.0(2)
O1–Na–O5	67.5(2)	68.5(1)	68.6(2)	69.9(1)

The conformation of the torsion angles N1–C8–C9–N2 and N2–C11–C12–N3 are g^- (−54.5°, mean value) and g^+ (+62.0°, mean value), respectively, and the direction of C10 is towards the convex part of the molecule, the same direction of Cl2 and the methanol bonded to the sodium ion. The coordination polyhedron around the sodium ion is a pentagonal pyramid, in which the six-coordinated oxygen atoms are from the O_2O_3 chamber of the macrocyclic ligand and from a methanol molecule placed at the vertex of the pyramid. The sodium atom is displaced by about 0.62 Å from the mean basal plane.

The conformations of the torsion angles O3–C21–C22–O4 and O4–C23–C24–O5 are g^+ and g^-, respectively, in all the complexes, and the values are between 50 and 55°. The contact distances Ln–Na present small variations around a mean value of 3.55 Å.

Solution structure: NMR spectra of diamagnetic complexes: The ^{13}C NMR spectrum of the diamagnetic complex $[YNa(L)(Cl)_2(CH_3OH)]$, recorded at 298 K and 75.4 MHz in CD_3OD, shows 12 resonances: five in the aliphatic region, due to the ethylenic and the methyl groups, and seven between 115 and 171 ppm, assigned to the aromatic and iminic carbon atoms (Figure 3, bottom). The resonances of the aliphatic carbons are assigned to the methyl group (42 ppm), to the methylenic carbons of the oxoethylenic bridges (67 and 69 ppm), and to the methylenic carbons of the N_3O_2 coordination site (57 and 58 ppm). The occurrence of such a simple spectral pattern is indicative of the presence in solution of a symmetry plane perpendicular to the molecule and passing through the Ln–Na axis. In the solid state, the complex has a lower symmetry, arising from the presence of a twist angle between the two aromatic rings of 41.52° (mean value) and the orientation of the methyl group directed towards one of the two halves of the molecule. Thus in methanolic solution there is a fluxional process that averages out pairs of carbon resonances. This dynamic behavior can be easily visualized as the result of a twisting motion of the two aromatic moieties.

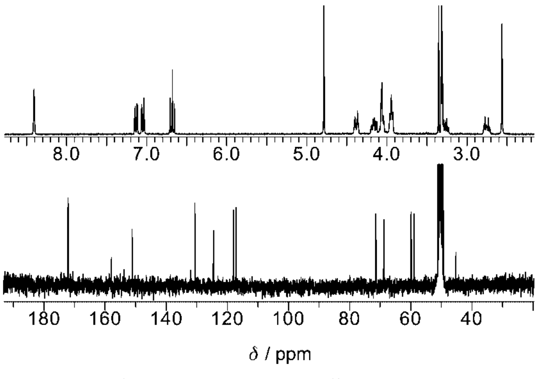

Figure 3. 300 MHz ^1H (top) and 75.4 MHz ^{13}C (bottom) NMR spectra of the diamagnetic complex $[YNa(L)]^{2+}$ in CD_3OD at 298 K.

This process has a low activation energy cannot be frozen out even at low temperature (233 K).

The corresponding ^{1}H NMR spectrum of the Y^{III} complex (300 MHz, 298 K) shows 11 resonances (Figure 3, top): a singlet at 8.4 ppm due to the iminic protons 4 (see Scheme 2), two doublets of doublets at 7.0 and 7.1 ppm attributed to the *meta* protons 2 and 3, a triplet at 6.7 ppm (1), six multiplets in the region 2.8–4.4 ppm, and a singlet at 2.6 ppm easily assigned to the methyl group 7. The presence of multiplets for the methylenic protons reveals a much higher degree of stereochemical rigidity for the heterodinuclear complexes as compared with the corresponding mononuclear ones, for which a time-averaged planar structure was present in methanolic solution.[25] This additional rigidity is provided by the coordination of the Na^{+} ion into the crown-ether site. A 400 MHz HMQC (heteronuclear multiple quantum coherence) experiment (298 K) allowed the correlation of the multiplets at 3.2 and 2.8 ppm with the ^{13}C resonance at 58 ppm, the multiplet at 3.9 ppm with the ^{13}C resonance at 57 ppm, the multiplet at 4.0 ppm with the ^{13}C resonance at 69 ppm, and the two multiplets at 4.1 and 4.4 ppm with the carbon peak at 67 ppm. Finally, a 2D NOESY ^{1}H experiment provided the basis for the complete assignment of the proton and carbon spectra. At 298 K and by using a mixing time of 280 ms, cross peaks were observed between the imino protons and the resonances at 7.0 and 3.9 ppm, which are then assigned to the protons 3 and 5, respectively, between the methyl group and the multiplets at 2.8 and 3.2 ppm (6), and between the proton 2 and the resonances at 4.1 and 4.4 ppm (9). The protons of the four ethylenic groups are in a staggered conformation and show a pattern consisting of two triplets of doublets (axial protons) and two doublets of doublets (equatorial). Interestingly, both the N_3O_2 and the O_3O_2 sites show a very similar multiplicity pattern, and this indicates that the conformation observed in the solid state is maintained in solution. Almost identical NMR spectra were observed for the corresponding Lu^{III} complex. Finally, in both the ^{1}H and ^{13}C NMR spectra only a single solvent peak is observed. This implies that in solution the two chloride anions are displaced by two solvent molecules that are in rapid exchange (on the NMR timescale) with the bulk of the solvent.

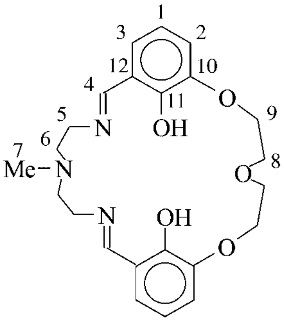

Scheme 2. Structure of the ligand with the labeling used to assign the resonances in the NMR spectra.

The spectra of the diamagnetic complexes do not provide a firm indication of the coordination sites occupied by the Ln^{III} and the Na^{+} ions and do not allow the assessment of structural changes in solution across the Ln^{III} series, as often observed.[20a, 34] These points may be conveniently addressed by considering the ^{1}H NMR spectra of the corresponding paramagnetic derivatives.

^{1}H NMR spectra of paramagnetic complexes: The ^{1}H NMR spectra were recorded in CD_3OD at 2.1 T for the paramagnetic complexes $[LnNa(L)]^{2+}$ (Ln = Ce, Pr, Nd, Sm, Eu, Tb, Dy, Ho, Er, Tm, Yb) (Figure 4).

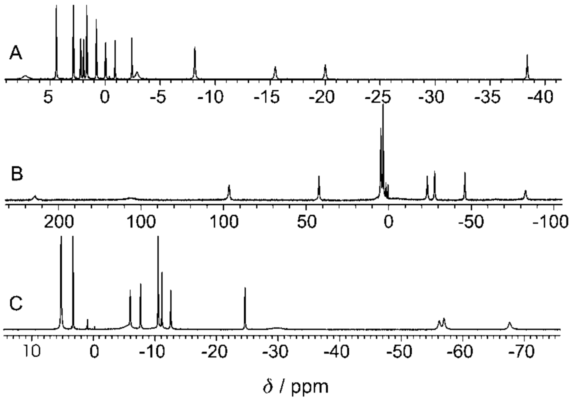

Figure 4. 300 MHz ^{1}H NMR spectra of the paramagnetic complexes $[LnNa(L)]^{2+}$ in CD_3OD at 298 K: Ln = Eu (A), Tb (B), and Yb (C).

All the spectra consist of 13 resonances and are characterized by very different chemical-shift ranges, from 11 ppm (Sm) to about 480 ppm (Dy), and different linewidths. Apart from one peak (methyl resonance, relative intensity 1.5), all the signals have an identical area (relative value 1), and this represents a strong limitation to the spectral assignment. However, some useful information can be inferred from a qualitative analysis of the spectra. The resonances can be divided into two different groups according to their different values of the bandwidth at half-height ($\Delta\nu_{1/2}$) and of the chemical shift:[35] i) six signals present chemical-shift values remarkably shifted from the diamagnetic spectral region and large bandwidths; ii) the second group of seven signals is characterized by values of δ and $\Delta\nu_{1/2}$, which are much closer to those typical of the diamagnetic derivatives. The resonances endowed with large values of both the isotropic paramagnetic shifts and the linewidths are associated with the protons in the proximity of the paramagnetic ion. Since the methyl group belongs to this set of peaks, we may assume that the Ln^{III} ion in solution is coordinated in the N_3O_2 Schiff-base compartment, as found in the solid state. A further proof of this conclusion was gained by calculating the average H–Ln distance for the methyl group by a well-established procedure, which exploits the quadratic magnetic field dependence of the Curie-spin relaxation mechanism.[36] For any magnetically active nucleus of the ligand in a complex of a paramagnetic lanthanide ion other than Gd, the paramagnetic contribution to the longitudinal relaxation rate is given by the following expression [Eq. (1)].

$$\frac{1}{T_{1p}} = R_{1p} = \frac{4}{15}\frac{\mu_B^2\gamma_H^2 g_J^2}{r_{LnH}^6} J(J+1)\tau_S + \frac{6}{5r_{LnH}^6(3KT)^2}\omega_H^2\mu_B^4 g_J^4 J^2(J+1)^2\tau_R \qquad (1)$$

ω_H and ω_S are the proton and electron Larmor frequencies, τ_S is the electron spin relaxation time (typically of the order of 0.1 ps), μ_B is the Bohr magneton, γ_I is the magnetogyric ratio of the nucleus I, g_J is the Landè factor, J is the total angular momentum of the lanthanide ion, and τ_R is the reorientational correlation time. The first term in Equation (1) represents the electron-nucleus dipolar interaction, whereas the second term refers to the Curie-spin relaxation mechanism, characterized by a quadratic dependence on the nuclear Larmor frequency. By plotting the longitudinal relaxation rates as a function of ω_H^2, a straight line is obtained, the slope of which allows the value of the Ln–H distance to be extracted, if τ_R can be independently estimated. The rotational correlation time, τ_R, can be conveniently calculated by a series of ^{13}C NMR experiments on a diamagnetic derivative. The protonated carbon atoms of the ligand relax mainly through a modulation of the dipolar interaction with the directly attached proton(s) with a correlation time given by τ_R [Eq. (2)].

$$R_1^{dd} = n\frac{4\gamma_C^2\gamma_H^2\eta^2 S(S+1)}{3r_{C-H}^6}\tau_r \quad (2)$$

In Equation (2), n is the number of hydrogen atoms bound to the carbon, γ_H and γ_C are the proton and carbon magnetogyric ratios, respectively, η is the Planck constant, r_{C-H} is the C–H distance, and S is the spin quantum number ($S = \tfrac{1}{2}$). Since the C–H distance for a methinic group is known to a high degree of accuracy ($r = 1.08$ Å), the value of τ_R can be derived from R_1^{dd}. The dipolar contribution to the relaxation rate, R_1^{dd}, is assessed by the measurements of the longitudinal relaxation rate (R_1^{obs}) and of the NOE factor (η) through the following expression [Eq. (3)].[37]

$$R_1^{obs}/R_1^{dd} = \eta_{max}/\eta \quad (3)$$

The ^{13}C $1/T_1$ value for the iminic carbon of the Y^{III} complex was found to be 2.0 s^{-1} at 300 K and 100.6 MHz, and the NOE factor was found to have the maximum value of 1.99.[37] From these data, a τ_R value of 88 ps is then calculated by assuming a C–H distance of 1.08 Å. Finally, longitudinal relaxation rates of 265, 320, and 388 s^{-1} were measured for the methyl resonance of the Yb^{III} complex at 90, 270, and 400 MHz (and at 300 K). By adopting the τ_R value previously calculated, we obtained from Equation (1) a distance r of 3.2 Å, in fairly good agreement with the value derived from crystallographic data. By following the same procedure, it was then possible to estimate the Yb–H distances associated with the other resonances of the ^{1}H NMR spectrum (see Supporting information). The calculated values confirm the previous qualitative analysis: a group of peaks corresponds to "short" distances of 3.0–4.0 Å (protons of the imino group and of the N_2O_3 site), whereas the other peaks correspond to "long" distances ranging from 4.8 to 6.0 Å (aromatic protons and protons of the O_2O_3 site).

In conclusion, all the NMR data indicate that the complexes from Nd to Yb maintain the same type of coordination polyhedron in methanolic solution as those found in the solid state, and thus this suggests a high degree of isostructurality across the series. This is in contrast to what has been observed for the corresponding mononuclear complexes, in which two rapidly interconverting isomeric species were present in solution for the Yb and Lu derivatives. This different behavior is likely to be associated with the high stereochemical rigidity imposed by the coordination of the Na$^+$ ion in the O_2O_3 crownlike binding site.

^{23}Na NMR spectra: The ^{23}Na NMR spectra, in CD_3OD at 298 K, of the Tb, Dy, Tm, and Yb complexes show the presence of a broad resonance characterized by a large shift from the peak of the free ion (Figure 5). This band is due to a Na$^+$ ion coordinated in the O_3O_2 site of the complexes which results in slow exchange at room temperature on the NMR timescale. The slow exchange is confirmed by the presence of a small peak at 0 ppm corresponding to the free ion (1–3 %) in the spectrum of the Tm complex; the peak originates from the coprecipitation of NaCl during the recrystallization of the complex. Upon addition of a small amount of NaCl to the methanolic solution of the complex, only an increase of this resonance is observed.

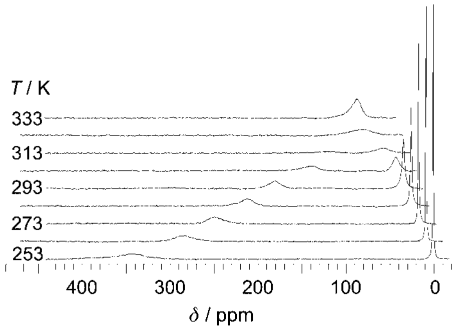

Figure 5. Variable-temperature 79.3 MHz ^{23}Na NMR spectra of $[TmNa(L)]^{2+}$ (ca. 20 mmol L^{-1}) in CD_3OD in the presence of added NaCl.

After increasing the temperature, the broad resonance sharpens and shifts downfield (upfield for the Tm complex). The exchange-averaged signal is observed only at temperatures above 320 K, and this indicates the strong binding of the sodium cation in the O_2O_3 site. A quantitative analysis of the spectra in order to obtain the kinetic parameters of the dynamic process was not attempted because of the predominant contribution of the paramagnetic relaxation to the bandwidth of the isotropically shifted signal at each temperature.

The observed isotropic shift is very large for all the three complexes and is positive for Tm and negative for Tb, Dy, and Yb (340, −614, −157, and −40 ppm, respectively, at 253 K). The magnitude of the ^{23}Na hyperfine shifts is a consequence of the very short Ln–Na distance found in these complexes as compared with those of the currently available shift reagents, in which the alkali-metal cations only form ion pairs with polar groups of the ligand.[20a, 34] This feature is very important for the development of ^{23}Na shift reagents of enhanced efficacy for the separation of the intra- and extracellular ^{23}Na resonances in biomedical studies.[20a] To this goal, future work will be directed to a suitable modification of the ligand in order to improve the water solubility of the complexes.

Another interesting aspect is the selectivity of this ligand for Na^{+} compared with other cations of the Groups I and II. We have addressed this problem by recording the ^{23}Na NMR spectra of the Ln–Na complexes (Ln = Tb, Dy, Tm, Yb) in the presence of equimolar amounts of LiCl, KBr, and $\mathrm{CaCl_2}$. The transmetalation reaction is revealed by the decrease in the intensity of the resonance of the bound Na^{+} cation and the appearance of the signal corresponding to the free Na^{+}. The reaction occurs, to a different extent, with all the three cations, and the binding affinity of the ligand follows the order $\mathrm{Ca}^{2+} > \mathrm{Na}^{+} \gg \mathrm{K}^{+} \gg \mathrm{Li}^{+}$. The high selectivity of the ligand for Ca^{2+} is probably due to an optimal fit of the ionic radius of the cation to the coordination site. It is possible that a chloride anion is coordinated to Ca^{2+} in order to maintain the electroneutrality, and this could also contribute to the stabilization of the complex. In order to check that the added cations only displace Na^{+} and not the lanthanide ion, we recorded the ^{1}H NMR spectra of the Tb–Na complex at 303 K in the presence of an equimolar amount of $\mathrm{CaCl_2}$. Under these conditions, we clearly see (Figure 6) a decrease in the intensity of the peaks associated with the Tb–Na complex and the appearance of a new set of resonances covering an almost identical chemical-shift range and easily attributable to the Tb–Ca complex. Hence, the transmetalation reaction does not involve the lanthanide cation.

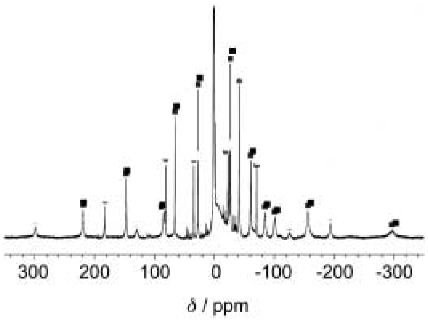

Figure 6. 90 MHz ^{1}H NMR spectrum of $[\mathrm{TbNa(L)}]^{2+}$ (15 mmol L^{-1}) in the presence of a twofold excess of $\mathrm{CaCl_2}$. The resonances attributed to the complex $[\mathrm{TbCa(L)}]^{3+}$ are labeled with ■.

Finally, we may anticipate that the complexes are expected to present good stability in water. When a small amount of water (four drops) is added to a methanolic solution (0.5 mL) of the Tb complex in the NMR tube, no changes are detected in the ^{1}H NMR spectrum over a period of three days. The corresponding ^{23}Na NMR spectra only show some line broadening as a function of the added water. This suggests that the $\mathrm{Ln^{III}}$ complexes will not dissociate in water and that the exchange between "free" and "bound" sodium cations will be accelerated, a favorable condition for possible in vivo applications.

Conclusion

We have prepared a series of stable $\mathrm{Na^{I}}$–$\mathrm{Ln^{III}}$ complexes with a macrocyclic ligand containing two adjacent cavities, a $\mathrm{N_3O_2}$ Schiff-base site, and a $\mathrm{O_2O_3}$ crown-ether-like site. The preference of Na^{+} for the polyoxa cavity is the key to the synthesis of well-defined, stable heterodinuclear Ln–Na complexes, in which Na^{+} resides in the $\mathrm{O_3O_2}$ chamber, and the $\mathrm{Ln^{III}}$ cation in the Schiff-base site. The complexes show a high degree of isostructurality both in methanolic solution and in the solid state. Furthermore, unlike the mononuclear complexes, the $[\mathrm{LnNa(L)(Cl)_2(CH_3OH)}]$ complexes are characterized in solution by a marked stereochemical rigidity as a consequence of the presence of two metal ions in the two adjacent coordination sites. The ^{23}Na NMR resonance of the bound cation is markedly shifted from that of the free ion by the paramagnetic $\mathrm{Ln^{III}}$ center. In the case of the Tb, Dy, and Tm complexes, the bound shifts are of the order of several hundreds ppm (in methanol), more than one order of magnitude greater than the corresponding values estimated (in water) for the shift reagents currently available.[20a, 38] The ^{23}Na paramagnetic shift depends upon the geometrical position of the sodium ion relative to the magnetic symmetry axis of the complex and upon the Ln–Na distance. Under the simplified hypothesis that the lanthanide complex is characterized by an effective axial symmetry (often a good approximation),[34] the magnitude of the shift is proportional to a term of the type $\mathrm{D_1}(3\cos^2\theta - 1)/r^3$, in which θ is the angle between the Ln–Na vector and the principal magnetic axis of the complex, and r is the Ln–Na distance. In the heterodinuclear Ln–Na complexes, the distance r is only approximately 3.55 Å, much shorter than that estimated for the corresponding polyaminopolycarboxylic (ca. 3.9 Å) and polyoxa tetraaza macrocyclic (5.3 Å) complexes.[39] Furthermore, the negative sign of the hyperfine ^{23}Na shifts for the Tb, Dy, and Yb complexes ($\mathrm{D_1} > 0$) suggests that the angle θ is close to 90°, and thus that the principal magnetic susceptibility axis of the complex is orthogonal to the molecular plane. This hypothesis is supported by the fact that in the ^{1}H NMR spectrum of the Yb complex (for which the dipolar contribution to the paramagnetic shift has the largest contribution) all the resonances have negative chemical-shift values (see Supporting Information).

At temperatures above approximately 40 °C, a fast exchange occurs between the "free" and "bound" sodium cations, and an average signal is observed. All these properties make the heterodinuclear Ln–Na complexes very promising candidates for the development of highly effective shift reagents for metal cations of biological importance.

Future work will be directed to the improvement of both the solubility of the complexes in water through a suitable modification of the ligand and the selectivity towards Na^{+} by changing the size of the crown-ether-like cavity.

Experimental Section

Materials: All the solvents, the reagents, and the lanthanide chlorides, $\mathrm{LnCl_3 \cdot \mathit{n}\,H_2O}$, were purchased from Aldrich and Fluka and used without further purification. Dimethylsulfoxide was distilled prior to use.[40]

Physico-chemical measurements: Elemental analyses were carried out by using a Fison 1108 analyzer. IR spectra were recorded as KBr pellets on a Mattson FTIR spectrometer. The ^{1}H and ^{13}C NMR spectra for the diamagnetic complexes were recorded on a Bruker AMX300 spectrometer equipped with a broad-band multinuclear probe and a variable-temperature unit. ^{23}Na NMR spectra were recorded on the same spectrometer with solutions (15–25 mmol L^{-1}) of the Ln^{III} complexes (Ln = Tb, Dy, Tm, Yb) in CD_3OD. Typically 2000 transients were necessary to obtain a satisfactory signal-to-noise ratio. The data were processed by using a line broadening of 20 Hz and a baseline correction. ^{23}Na chemical shifts were measured in relation to the ^{23}Na signal of a solution of NaCl (5 M) in CD_3OD. Downfield-induced shifts are denoted as positive. The chemical shifts (^{23}Na) and the peak widths were determined by fitting the signals to a Lorenzian line function. 2D NOESY and HMQC experiments for the diamagnetic complexes were performed on a Bruker AVANCE 400 spectrometer. ^{1}H NMR spectra of the paramagnetic complexes were recorded at 0, 30, and 60 °C on a JEOL EX-90 spectrometer operating at 2.1 T. All the samples examined were dissolved in deuterated methanol used also as an internal reference. The T_1 longitudinal relaxation times were measured on JEOL EX90, EX270, and EX400 spectrometers (operating at 2.1, 6.4, and 9.4 T, respectively) at 30 °C by using the standard inversion recovery pulse sequence.

The morphology, homogeneity, and the metal/chlorine ratio of the complexes were investigated by using a Philips XL40 model scanning electron microscope equipped with an EDAX DX PRIME X-ray energy dispersive spectrometer.[41] The solvent content (H_2O or MeOH) was evaluated by thermal analysis curves by using Netzsch STA 429 thermoanalytical equipment. The tests were performed under a nitrogen atmosphere (flux rate 250 mL min^{-1}; heating rate 5 °C min^{-1}) and in air under the same conditions. Neutral alumina (Carlo Erba, Milano, Italy) was used as reference material. All mass spectrometric measurements were performed on a VG ZAB 2F instrument (VG Analytical Ltd.) operating under fast-atom-bombardment (FAB) conditions (8 keV Xe atoms bombarding a solution of the sample in nitrobenzyl alcohol). Also ESI-MS spectra have been recorded by using a Finnigan LCQ mass spectrometer and methanolic solutions of the samples (10^{-5} M).[42]

Preparation of H_2L' and Na_2L': The diformyl precursor 3,3′-(3-oxapentane-1,5-diyldioxy)bis(2-hydroxybenzaldehyde) (H_2L') and the disodium derivative (Na_2L') were prepared by a modification of the literature procedure.[25, 27, 29]

Preparation of H_2L: A methanolic solution (3 mL) of 1,5-diamino-3-azamethylpentane (5 mmol) was diluted with diethyl ether (300 mL). A solution (5 mL) in $CHCl_3$ of the diformyl precursor 3,3′-(3-oxapentane-1,5-diyldioxy)bis(2-hydroxybenzaldehyde) (5 mmol) was added dropwise at room temperature. The yellow precipitate was stirred for 15–20 min, then filtered, washed twice with a solution in diethyl ether/methanol, and dried in vacuum. The yellow compound was identical to that prepared by other methods reported in the recent literature.[25, 27]

^{1}H NMR (300 MHz, $CDCl_3$, 25 °C, TMS): $\delta = 8.19$ (s, 2H; CNH), 6.75 (m, 6H; Ar–H), 4.20 (m, 4H; CH_2O), 3.95 (m, 4H; CH_2O), 3.63 (m, 4H; $CNCH_2$), 2.78 (m, 4H; CH_2NCH_3), 2.32 (s, 3H; CH_3); elemental analysis calcd (%) for $C_{23}H_{29}N_3O_5 \cdot H_2O$: C 62.71, H 6.73, N 9.28; found: C 62.01, H 7.01, N 9.43.

Preparation of Na_2L: The compound 1,5-diamino-3-azamethylpentane (15 mmol) in methanol (10 mL) was added dropwise to a methanolic solution (150 mL) of the disodium salt of 3,3′-(3-oxapentane-1,5-diyldioxy)bis(2-hydroxybenzaldehyde) (15 mmol). The brown solution was refluxed for 2 h until a yellow precipitate was formed. It was collected by filtration, washed twice with methanol and diethyl ether, and dried in vacuo.

^{1}H NMR (300 MHz, $CDCl_3$, 25 °C, TMS): $\delta = 8.15$ (s, 2H; CNH), 6.74 (d, 2H; Ar–H), 6.50 (d, 2H; Ar–H), 6.21 (t, 2H; Ar–H), 3.96 (m, 4H; CH_2O), 3.50 (m, 4H; $CNCH_2$), 3.48 (m, 4H; CH_2O), 3.10 (m, 4H; CH_2NCH_3), 2.29 (s, 3H; CH_3); elemental analysis calcd (%) for $C_{23}H_{27}N_3O_5Na_2$: C 58.60, H 5.77, N 8.91; found: C 58.36, H 5.69, N 8.38.

Preparation of $[LnNa(L)(Cl)_2(CH_3OH)]$ (Ln = Y, La, Ce, Nd, Sm, Eu, Gd, Tb, Dy, Ho, Er, Tm, Yb, Lu): Two alternative methods were used: a) the appropriate lanthanide trichloride hydrate, $LnCl_3 \cdot nH_2O$ (1 mmol), and 1,5-diamino-3-azamethylpentane (1 mmol) in methanol (10 mL) were added in succession to a methanolic solution (30 mL) of the disodium derivative of the diformyl precursor 3,3′-(3-oxapentane-1,5-diyldioxy)bis(2-hydroxybenzaldehyde) (Na_2L', 1 mmol). The resulting yellow solution was refluxed for 3 h. The solvent was evaporated to dryness under reduced pressure, and the yellow residue was treated twice with ethanol (30 mL) (for the Lu, Nd, and Ce complexes *n*-propanol was used), filtered, washed with diethyl ether, and dried in vacuo. A yellow powder was obtained which was recrystallized by slow diffusion of diethyl ether in a solution in methanol to yield well-formed yellow crystals suitable for X-ray analysis; b) NaOH (2 mmol) in methanol (10 mL) and $LnCl_3 \cdot nH_2O$ (1 mmol) in methanol (30 mL) were added in succession to a methanolic solution (50 mL) of the macrocycle H_2L (1 mmol). The resulting yellow solution was refluxed for 3 h and then evaporated to dryness. The yellow residue was washed twice with ethanol and diethyl ether (for the Lu, Nd, and Ce complexes *n*-propanol was used). The resulting yellow powder was recrystallized as in method a.

$[LaNa(L)(Cl)_2(CH_3OH)]$: IR (KBr): $\tilde{\nu} = 1632$ cm^{-1} (C=N); elemental analysis calcd (%) for $[LaNa(L)(Cl)_2(CH_3OH)]$: C 41.76, H 4.53, N 6.09; found: C 41.16, H 4.41, N 5.44.

$[YNa(L)(Cl)_2(CH_3OH)]$: IR (KBr): $\tilde{\nu} = 1626$ cm^{-1} (C=N); elemental analysis calcd (%) for $[YNa(L)(Cl)_2(CH_3OH)]$: C 45.02, H 4.88, N 6.56; found: C 45.27, H 5.04, N 6.49.

$[LuNa(L)(Cl)_2(CH_3OH)]$: IR (KBr): $\tilde{\nu} = 1628$ cm^{-1} (C=N); elemental analysis calcd (%) for $[LuNa(L)(Cl)_2(CH_3OH)]$: C 39.69, H 4.30, N 5.78; found: C 40.00, H 4.36, N 5.67.

$[YbNa(L)(Cl)_2(CH_3OH)]$: IR (KBr): $\tilde{\nu} = 1628$ cm^{-1} (C=N); elemental analysis calcd (%) for $[YbNa(L)(Cl)_2(CH_3OH)]$: C 39.79, H 4.31, N 5.80; found: C 39.05, H 4.26, N 5.61.

$[TmNa(L)(Cl)_2(CH_3OH)]$: IR (KBr): $\tilde{\nu} = 1627$ cm^{-1} (C=N); elemental analysis calcd (%) for $[TmNa(L)(Cl)_2(CH_3OH)]$: C 40.02, H 4.34, N 5.83; found: C 40.14, H 3.95, N 5.59.

$[EuNa(L)(Cl)_2(CH_3OH)]$: IR (KBr): $\tilde{\nu} = 1631$ cm^{-1} (C=N); elemental analysis calcd (%) for $[EuNa(L)(Cl)_2(CH_3OH)]$: C 40.98, H 4.44, N 5.97; found: C 40.95, H 4.29, N 5.93.

$[NdNa(L)(Cl)_2(CH_3OH)]$: IR (KBr): $\tilde{\nu} = 1620$ cm^{-1} (C=N); elemental analysis calcd (%) for $[NdNa(L)(Cl)_2(CH_3OH)]$: C 41.44, H 4.49, N 6.04; found: C 40.60, H 4.20, N 5.83.

$[CeNa(L)(Cl)_2(CH_3OH)]$: IR (KBr): $\tilde{\nu} = 1617$ cm^{-1} (C=N); elemental analysis calcd (%) for $[CeNa(L)(Cl)_2(CH_3OH)]$: C 41.89, H 4.13, N 6.37; found: C 40.73, H 4.10, N 6.48.

$[SmNa(L)(Cl)_2(CH_3OH)]$: IR (KBr): $\tilde{\nu} = 1629$ cm^{-1} (C=N); elemental analysis calcd (%) for $[SmNa(L)(Cl)_2(CH_3OH)]$: C 39.41, H 4.43, N 5.95; found: C 39.17, H 3.78, N 5.72.

$[TbNa(L)(Cl)_2(CH_3OH)]$: IR (KBr): $\tilde{\nu} = 1619$ cm^{-1} (C=N); elemental analysis calcd (%) for $[TbNa(L)(Cl)_2(CH_3OH)]$: C 40.58, H 4.40, N 5.92; found: C 41.00, H 4.32, N 5.88.

$[HoNa(L)(Cl)_2(CH_3OH)]$: IR (KBr): $\tilde{\nu} = 1623$ cm^{-1} (C=N); elemental analysis calcd (%) for $[HoNa(L)(Cl)_2(CH_3OH)]$: C 40.37, H 3.98, N 6.14; found: C 39.82, H 3.36, N 6.35.

$[GdNa(L)(Cl)_2(CH_3OH)]$: IR (KBr): $\tilde{\nu} = 1625$ cm^{-1} (C=N); elemental analysis calcd (%) for $[GdNa(L)(Cl)_2(CH_3OH)]$: C 40.83, H 4.02, N 6.21; found: C 41.01, H 4.03, N 6.26.

$[DyNa(L)(Cl)_2(CH_3OH)]$: IR (KBr): $\tilde{\nu} = 1621$ cm^{-1} (C=N); elemental analysis calcd (%) for $[DyNa(L)(Cl)_2(CH_3OH)]$: C 40.38, H 4.38, N 5.89; found: C 39.98, H 4.15, N 6.08.

$[ErNa(L)(Cl)_2(CH_3OH)]$: IR (KBr): $\tilde{\nu} = 1625$ cm^{-1} (C=N); elemental analysis calcd (%) for $[ErNa(L)(Cl)_2(CH_3OH)]$: C 39.52, H 3.89, N 6.01; found: C 38.42, H 3.63, N 5.12.

X-ray crystallography: Diffraction data were collected at room temperature on a Philips PW1100 automatic four-circle diffractometer (FEBO System) using graphite-monochromated $Mo_{K\alpha}$ radiation and the $\omega - 2\theta$ scan method. Lattice parameters were obtained from a least-squares refinement of the setting angles of 30 reflections with $12 \leq 2\theta \leq 25°$. Table 2 lists a summary of the crystallographic data and structure refinement. No sign of crystal deterioration was revealed when monitoring three standard reflections every 200 measurements. The structures were solved by standard Patterson methods and subsequently completed by a combination of least-squares techniques and Fourier syntheses with the SHELX program.[43] All the benzene rings were refined as rigid bodies, the hydrogen atoms were included in the idealized positions with fixed C–H distances (C–H = 1.08 Å), and isotropic temperature factors fixed to 1.2 times U(eq) of the preceding carbon or nitrogen atom.

The asymmetric unit of all the compounds contained, coordinated to the sodium ion, a disordered methanol molecule with two different positions of the oxygen atom, refined to final values of about 20 and 80%. Listings of selected bond lengths and angles pertinent to the coordination polyhedron are summarized in Table 2 and Table 3. Additional crystallographic data, atomic coordinates, anisotropic thermal parameters, and full listings of bond lengths and angles have been deposited with CCDC.

CCDC 172972–172975 contain the supplementary crystallographic data for this paper. These data can be obtained free of charge via www.ccdc.cam.ac.uk/conts/retrieving.html (or from the Cambridge Crystallographic Data Centre, 12 Union Road, Cambridge CB21EZ, UK; fax: (+44)1223-336-033; or e-mail: deposit@ccdc.cam.ac.uk).

Acknowledgements

The authors would like to thank Mr. Aguiari, Mrs. Biolo, and Mrs. Moresco for experimental assistance and CNR ("MURST-CHIMICA" Legge 95/95) for financial support.

---

[1] D. Alexander, *Coord. Chem. Rev.* **1995**, *95*, 273.

[2] P. Guerriero, S. Tamburini, P. A. Vigato, *Coord. Chem. Rev.* **1995**, *95*, 17.

[3] P. Guerriero, P. A. Vigato, D. E. Fenton, P. C. Hellier, *Acta Chem. Scand.* **1992**, *46*, 1025.

[4] J. Nelson, V. McKee, G. Morgan in *Progress in Inorganic Chemistry, Vol. 47* (Ed.: K. D. Karlin), Wiley, New York, **1988**, p. 167, and references therein.

[5] a) D. M. Rudkevich, J. D. Mercer-Chalmers, W. Verboom, R. Ungaro, F. de Jong, D. N. Reinhoudt, *J. Am. Chem. Soc.* **1995**, *117*, 6124; b) D. M. Rudkevich, Z. Brozka, M. Palys, C. H. Visser, W. Verboom, D. N. Reinhoudt, *Angew. Chem.* **1994**, *106*, 480; *Angew. Chem. Int. Ed. Engl.* **1994**, *33*, 467; c) D. M. Rudkevich, W. Verboom, D. N. Reinhoudt, *J. Org. Chem.* **1994**, *59*, 3683; d) D. M. Rudkevich, W. P. R. V. Stauthamer, J. F. J. Engbersen, S. Harkema, D. N. Reinhoudt, *J. Am. Chem. Soc.* **1992**, *114*, 9671; e) D. M. Rudkevich, W. Verboom, Z. Brozka, M. Palys W. P. R. V. Stauthamer, G. J. van Hummel, S. M. Franken, S. Harkema, J. F. J. Engbersen, D. N. Reinhoudt, *J. Am. Chem. Soc.* **1994**, *116*, 4341.

[6] K. S. Murray in *Advances in Inorganic Chemistry, Vol. 43* (Ed.: A. G. Sikes), Academic Press, San Diego, **1995**, p. 261.

[7] O. Kahn in *Advances in Inorganic Chemistry, Vol. 43* (Ed.: A. G. Sikes), Academic Press, San Diego, **1995**, p. 179.

[8] D. E. Fenton in *Advances in Inorganic and Bioinorganic Mechanism, Vol. 43* (Ed.: A. G. Sikes), Academic Press, London, **1983**, p. 187.

[9] P. Zanello, S. Tamburini, P. A. Vigato, G. A. Mazzocchin, *Coord. Chem. Rev.* **1987**, *77*, 165.

[10] a) U. Casellato, P. A. Vigato, D. E. Fenton, M. Vidali, *Chem. Soc. Rev.* **1979**, *8*, 199; b) P. A. Vigato, S. Tamburini, D. E. Fenton, *Coord. Chem. Rev.* **1990**, *106*, 25; c) D. E. Fenton, P. A. Vigato, *Chem. Soc. Rev.* **1988**, *17*, 89.

[11] F. L. Urbach in *Metal Ions in Biological Systems. Copper Proteins No. 13* (Ed.: H. Siegel), Marcel Dekker, Basel, **1981**, p. 73, and references therein.

[12] T. M. Sorrel, *Tetrahedron* **1989**, *45*, 3.

[13] Q. Y. Chen, R.-H. Luo, Z.-L. Wang, J.-T. Chen, *Chem. Commun.* **2000**, 1033.

[14] J. Lisowski, *Inorg. Chim. Acta* **1999**, *285*, 233.

[15] H. He, A. E. Martell, R. J. Motekaitis, J. L. Reibenspies, *Inorg. Chem.* **2000**, *34*, 1586.

[16] H. Okawa, H. Furutacki, D. E. Fenton, *Coord. Chem. Rev.* **1998**, *174*, 51.

[17] D. G. McCollum, D. Bosnich, *Inorg. Chim. Acta* **1998**, *270*, 13.

[18] U. Casellato, P. Guerriero, S. Sitran, P. A. Vigato, C. Marega, A. Marigo, R. Zannetti, *Inorg. Chim. Acta* **1990**, *171*, 103.

[19] M. Yonemura, Y. Matsamura, H. Furutachi, M. Ohba, H. Okawa, D. E. Fenton, *Inorg. Chem.* **1997**, *36*, 2711.

[20] a) A. D. Sherry, C. F. G. C. Geraldes in *Lanthanide Probes in Life, Chemical and Earth Sciences* (Eds.: J.-C. G. Bünzli, G. R. Choppin), Elsevier, Amsterdam, **1989**, Chapter 4; b) K. O. A. Chin, J. R. Morrow, C. H. Lake, M. R. Churchill, *Inorg. Chem.* **1994**, *33*, 656; c) N. Sabatini, M. Guardigli, J.-M. Lehn, *Coord. Chem. Rev.* **1993**, *123*, 201.

[21] C. Benelli, A. Caneschi, D. Gatteschi, L. Pardi, *Mater. Chem. Phys.* **1992**, *31*, 17.

[22] N. Brianese, U. Casellato, S. Tamburini, P. Tomasin, P. A. Vigato, *Inorg. Chim. Acta* **1998**, *272*, 235.

[23] A. Aguiari, N. Brianese, S. Tamburini, P. A. Vigato, *New J. Chem.* **1995**, *262*, 627.

[24] U. Casellato, S. Tamburini, P. Tomasin, P. A. Vigato, *Inorg. Chim. Acta* **1997**, *262*, 117.

[25] U. Casellato, S. Tamburini, P. Tomasin, P. A. Vigato, S. Aime, M. Botta, *Inorg. Chem.* **1999**, *38*, 2906.

[26] M. D'Alpaos, S. Tamburini, P. Tomasin, P. A. Vigato, P. Traldi, *Rapid Commun. Mass Spectrom.* **1997**, *11*, 1909.

[27] N. Brianese, U. Casellato, S. Tamburini, P. Tomasin, P. A. Vigato, *Inorg. Chem. Commun.* **1999**, *2*, 149.

[28] N. Brianese, U. Casellato, S. Tamburini, P. Tomasin, P. A. Vigato, *Inorg. Chim. Acta* **1999**, *293*, 178.

[29] a) C. J. van Staveren, J. van Eerden, F. C. J. M. van Veggel, S. Harkema, D. N. Reinhoudt, *J. Am. Chem. Soc.* **1988**, *110*, 4994; b) F. C. J. M. van Veggel, M. Bos, S. Harkema, W. Verboom, D. N. Reinhoudt, *Angew. Chem.* **1989**, *101*, 800; *Angew. Chem. Int. Ed. Engl.* **1989**, *28*, 746; c) F. C. J. M. van Veggel, M. Bos, S. Harkema, H. van de Bovenkamp, W. Verboom, J. Reedijk, D. N. Reinhoudt, *J. Org. Chem.* **1991**, *56*, 22.

[30] C. S. Springer, Jr., *Am. Rev. Biophys. Chem.* **1987**, *16*, 375.

[31] *Cation Binding by Macrocycles* (Eds.: Y. Inoue, G. W. Gokel), Marcel Dekker, New York, **1990**.

[32] *Crown Compounds: Toward Future Applications* (Ed.: S. R. Cooper), VCH, Weinheim, **1992**.

[33] U. Casellato, S. Tamburini, P. Tomasin, P. A. Vigato, S. Aime, A. Barge, M. Botta, *Chem. Commun.* **2000**, 145.

[34] J. A. Peters, J. Huskens, D. J. Raber, *Prog. Nucl. Magn. Reson. Spectrosc.* **1996**, *28*, 283.

[35] I. Bertini, C. Luchinat, *NMR of Paramagnetic Substances, Coord. Chem. Rev. 150*, Elsevier, Amsterdam, **1996**, p. 1.

[36] a) S. Aime, L. Barbero, M. Botta, G. Ermondi *J. Chem. Soc. Dalton Trans.* **1992**, 225; b) L. Banci, I. Bertini, C. Luchinat, *Nuclear and Electron Relaxation*, VCH, Weinheim, **1991**.

[37] R. K. Harris, *Nuclear Magnetic Resonance Spectroscopy*, Longman, Harlow, **1986**.

[38] a) R. B. Hutchinson, J. I. Shapiro, *Concepts Magn. Reson.* **1991**, *3*, 215; b) C. S. Springer, Jr., in *NMR Techniques in the Study of Cardiovascular Structure and Function* (Eds.: M. Osbakken, J. Haselgrove), Futura Publishing, New York, **1988**, Chapter 4.

[39] R. M. Sink, D. C. Buster, A. D. Sherry, *Inorg. Chem.* **1990**, *29*, 3645.

[40] D. D. Perrin, W. L. Armarego, D. R. Perrin in *Purification of Laboratory Chemicals*, 2nd ed., Pergamon Press, Oxford, **1982**.

[41] P. Guerriero, P. A. Vigato, B. Burtet-Fabris, *Inorg. Chim. Acta* **1989**, *164*, 155.

[42] a) P. P. Morgan, J. M. Beynon, R. M. Bateman, B. M. Green, *Int. J. Mass Spectrom. Ion Processes* **1978**, *28*, 171; b) M. Barber, R. S. Bordoli, R. D. Sedgwick, A. M. Taylor, *J. Chem. Soc. Chem. Commun.* **1981**, *7*, 171.

[43] a) *SHELX-86 Crystallographic Computing 3* (Eds.: G. M. Sheldrick, C. Kruger, R. Goddard), Oxford University Press, London, **1985**, p. 175; b) G. M. Sheldrick, SHELXL-93, Program for Crystal Structure Refinement, University of Göttingen, Göttingen (Germany), **1993**.

Received: December 3, 2001 [F3720]